Backstepping-Based Cascade Control Scheme for Batch Distillation Columns

Rosendo Monroy-Loperena
Ingeniería Molecular, Instituto Mexicano del Petróleo, 07730 Distrito Federal, Mexico

Jose Alvarez-Ramirez
Departamento de Ingeniería de Procesos e Hidráulica, Universidad Autónoma Metropolitana-Iztapalapa, 09340 Distrito Federal, Mexico

DOI 10.1002/aic.10184
Published online in Wiley InterScience (www.interscience.wiley.com).

Nonstationary dynamics, finite-time operation, large thermodynamical uncertainty and delayed composition measurements make the control of batch distillation processes a challenging and interesting problem. In this paper, a cascade control design to regulate the overhead composition of a batch distillation column is presented. The controller is designed within the framework of robust nonlinear control with modeling error compensation techniques in conjunction with a backstepping approach. The result is a cascade controller with a master loop that, driven by the composition regulation error, produces a time-varying set point for the temperature in a certain tray; and with a secondary controller that manipulates the internal reflux ratio to track the time-varying set point determined by the master composition loop. How to extend the controller design to have multiple slave temperature controllers, to improve the regulation of the overhead composition in a batch distillation column, is also presented. The proposed control approach is illustrated by numerical simulations on a full dynamical model. © 2004 American Institute of Chemical Engineers *AIChE J,* 50: 2113–2129, 2004
Keywords: batch distillation, composition control, backstepping design, cascade control, low gain, high gain

Introduction

Batch distillation is a flexible separation processes that are becoming widely used. The main reason is that production amounts are usually small with minimum raw material inventories; this often results in an economic incentive (Barolo and Berto, 1998; Diwekar, 1991). Compared to continuous distillation, batch distillation offers flexible and economically attractive options for equipment reduction because the same equipment can be used for different products depending on market demand.

Recent trends in batch distillation control research focus on the development of efficient feedback control configurations. Within the control theory framework, the problem can be formulated as a tracking problem where an optimal temperature or composition profile becomes the reference trajectory for a feedback controller (Quintero-Marmol et al., 1991). The flexibility offered by batch distillation, however, gives rise to challenging control problems that are attributed to the nonstationary, nonlinear, and finite-time duration nature of the underlying dynamics. Because in a batch distillation operation there is no steady state, there is no normal condition at which traditional input/output linear models can be constructed and controllers can be tuned. Accordingly, satisfactory control responses have thus far not been obtained (Kim, 1999; Quintero-Marmol et al., 1991). Moreover, it is recognized that traditional

Correspondence concerning this article should be addressed to R. Monroy-Loperena at r.monroy-loperena@imp.mx.

proportional integral/proportional integral derivative (PI/PID) controllers, which perform quite well for continuous distillation, provide poor performance because of the nonstationary nature of batch distillation.

To address the control problem for batch distillation, several design methodologies have been proposed. Quintero-Marmol et al. (1991) proposed an inferential control scheme where composition is estimated through an extended Luenberger observer. Fileti and Rocha-Pereira (1997) (see also Bosley and Edgar, 1993) used gain-scheduled PI control for binary batch distillation. In their approach, the controller gain is increased during operation in order to keep maintaining the control goal. Predictive and adaptive control schemes have been proposed to confront the time-varying nature of the batch distillation process. Li and Wozny (2001) proposed that a predefined optimal policy can be tracked by an adaptive control strategy, to realize the optimum of multiple-fraction batch distillation. In their approach, a recursive least-square estimation with a variable forgetting factor is applied to the on-line identification of the plant to follow the changing dynamics of the process. Dechechi et al. (1998) showed that nonlinear model predictive control yields good results for distillate composition regulation. Their strategy requires that an extended Luenberger observer coupled with an optimization problem be solved on-line, which can lead to very complex controllers (Barolo and Berto, 1998). Barolo and Berto (1998) used nonlinear control theory (Henson and Seborg, 1997) to construct controllers for distillate composition in batch distillation. Their idea is to use input/output linearizing feedback control coupled with composition estimation (Quintero-Marmol et al., 1991), resulting in a nonlinear inferential control structure. Alvarez-Ramirez et al. (2000) used a modeling error–compensation technique to counteract the effects of model/plant mismatches, by means of an observer-based estimation of the modeling error. Their control design approach leads to a classical PID control with antireset windup scheme with guaranteed closed-loop stability.

A drawback of these approaches is that they strongly rely on an accurate model of the batch distillation process. For instance, methodologies that use nonlinear control theory require an accurate model because the construction of the underlying feedback controller uses exact cancellation of nonlinearities. Batch distillation models suffer from serious uncertainty because of poor knowledge of the thermodynamics of the mixtures. On the other hand, composition measurements can be expensive and time-delayed. In turn, these situations can lead to serious robustness and performance problems of the controlled batch distillation column. In particular, delayed control inputs can be ineffective because of the finite-time duration of the batch distillation process (that is, the desired composition trajectory is achieved at the end of the process).

From a practical viewpoint, it would be desirable to dispose of measurement-driven, simple linear controllers giving good performance and stability margin. There are many reasons for this, including their long history of proven operation and that they are well understood by many industrial operational, technical, and maintenance individuals. Besides, in many applications, a properly designed and well-tuned linear controller must meet or exceed the control objectives. Because accurate models of batch distillation are rarely available in industrial applications, such linear controllers should be computed from simple input/output models obtained from reliable plant data, for instance.

Compared to what is currently in the literature (see, for example, Alvarez-Ramirez et al., 2000; Barolo and Berto, 1998; Oisiovici and Cruz, 2001; Quintero-Marmol et al., 1991), our contribution can be summarized as follows:

(1) Based on an open-loop test to identify the batch distillation process (BDP) coupled with a backstepping approach (see, for example, Krstic et al., 1995), a robust cascade controller to regulate the overhead composition of a batch distillation column (BDC) is proposed. Specifically, the overall controller is composed of two cascade control loops. The primary control loop is basically a low-gain controller, which uses slow (delayed) composition measurements to provide servo responses (compositional control). The secondary control loop has the structure of a high-gain first-order integrator, which uses fast temperature measurements at a given distillation tray to *track* the output of the primary controller.

(2) Systematic extensions for multicascade control configuration are obtained as a natural consequence of the backstepping design procedure.

(3) Reliable tuning guidelines are provided in terms of a desired closed-loop performance.

The results in this work should be seen as the first reliable linear control to regulate the overhead composition of a BDP, even in the case where the distillate composition is measured or inferred with time-delay.

Identification of Simple Input/Output Linear Models for Batch Distillation

The basic mathematical model for the description of a BDP is a large (structured) system of differential-algebraic equations of the form (see Appendix)

$$\mathbf{f}(\dot{\mathbf{x}}, \mathbf{x}, t, \mathbf{u}) = \mathbf{0}, \; t \in [0, t_f]$$

where t denotes time, t_f is the batch period, $\mathbf{x}$ is the vector of state variables (such as flows, concentrations, pressures, temperatures, etc.), whereas $\mathbf{u}$ denotes the vector of manipulated variables (such as reflux flow, tray temperature, etc.). Schematically, a typical operation of a BDC can be described as follows. The mixture is added into the reboiler drum, and certain distillate composition, $x_{i,1}$, denoted as y, is made to track a prescribed (commonly optimal) trajectory $y_r(t)$ by manipulating the reflux ratio, L_1, denoted as u. At first, the distillate composition $y(t)$ starts from the initial condition $y(0)$, such that a control policy must ensure composition tracking in the sense that $y(t) \rightarrow y_r(t)$ as close and as soon as possible. Quick trajectory tracking is of prime importance for the successful operation of batch distillation columns because the processes duration is finite (of the order of hours). As discussed in the introduction, in the BDP operation there is no steady state, so there is no normal condition at which a linear input/output model can be constructed by step- or frequency-response methods. On the other hand, a control design based on a full mathematical model of the column has serious drawbacks, such as very complex nonlinear control structures that require measurements of a large set of signals (compositions, temperatures, and flow rates) and fragile controllers resulting from the large amount of uncertainties (Alvarez-Ramirez et al.,

2000; Barolo and Berto, 1998; Oisiovci and Cruz, 2001; Quintero-Marmol et al., 1991). In the following, simple input/output linear models and their identification procedure are described. The idea is to have simple models to be used for robust control design.

In the continuous distillation process, one can use step responses to obtain an input/output model of the dynamics. In general, such dynamical response can be approximated with two time constants plus a time-delay stable model as follows (Morari and Zafiriou, 1989)

$$\frac{y(s)}{u(s)} = G(s) = \frac{K_{ss}}{(\tau_1 s + 1)(\tau_2 s + 1)} \tag{1}$$

where K_{ss} is the steady-state gain, τ_1 is a time-constant related to the internal flow dynamics, and τ_2 is a time constant corresponding to external flow dynamics. For continuous distillation, the step response to obtain the model $y(s) = G(s)u(s)$ is made at the nominal operating conditions, which corresponds to a *steady-state operating point*. Once the input/output model (Eq. 1) is available, one can use, for instance, an internal model control–tuning approach to obtain a suitable PI/PID controller with guaranteed stability and performance properties (Morari and Zafiriou, 1989). By continuity, the model in Eq. 1 can be still used to design feedback controller at operating conditions near the nominal operating point. Extensive studies on the problem of robustness of control for continuous distillation is available in the chemical engineering literature. However, when designing a feedback controller for the batch distillation process one confronts the problem that the column does not operate at a steady-state operating point. Instead, the BDP operation is made along a dynamical trajectory induced by changing composition conditions in the reboiler drum. This implies that there is no a nominal operating point at which a stationary model like that expressed in Eq. 1 can be constructed. Based on this fact, one realizes that dynamical behavior of batch distillation is of a nature different from that of the dynamics of continuous distillation. The main difference relies on the fact that, whereas continuous distillation operates around a steady-state point, batch distillation operates along a nonstationary trajectory.

As mentioned earlier, using a full rigorous mathematical model to design a practical feedback controller for BDP has several drawbacks, including robustness problems because of uncertainties (such as thermodynamics, internal flows, etc.) and lack of stage composition and flow measurements (Kim, 1999; Quintero-Marmol et al., 1991). As in continuous distillation, an alternative is to use simple input/output models, which retain the main characteristics of the process dynamics for control design. Indeed, the main characteristic to be retained is the absence of a steady-state operating point. If $y(s) = G(s)u(s)$ is the representation of the BDP input/output model, the above requirement implies that $\lim_{s\to 0} |G(s)| = \infty$. That is, the process has no finite steady-state gain. To see that infinite steady-state gain is necessary, assume that $|G(0)| = \gamma < \infty$. This would imply that $y(s) = \gamma u(s)$ as $s \to 0$. Consequently, the output $y(t)$ would achieve a steady-state value (recall that $s \to 0$ is equivalent to $t \to \infty$). This is a contradiction to the fact that the operation of the batch process has no a steady-state operating point.

The requirement $\lim_{s\to 0} |G(s)| = \infty$ imposes a constraint in the class of input/output transfer functions for the batch distillation dynamics. In particular, such a requirement implies that the transfer function $G(s)$ must have at least one pole at the origin. That is, $G(s)$ can be written as

$$G(s) = \frac{1}{s^n} G^*(s)$$

where n is the number of poles at the origin and $G^*(s)$ is a transfer function with no poles at the origin (that is, $|G^*(0)|$ is finite). In particular, in a manner similar to the continuous distillation case, $G^*(s)$ can be taken as a stable transfer function with two time constants

$$G^*(s) = \frac{K_{uy}}{(\tau_1 s + 1)(\tau_2 s + 1)}$$

where K_{uy} is a given process gain. In this way, one can see the batch distillation dynamics as composed of a stable dynamics $G^*(s)$ filtered with an nth-order integrator. A physical interpretation of this transfer function configuration can be given as follows: At small time scales, the BDP can be seen as a stationary (continuous-like) distillation process operating at the existing boiler drum composition conditions. These small time-scale dynamics can be modeled by the stable transfer function $G^*(s)$ (Morari and Zafiriou, 1989). Given the operating nature of the batch distillation, the existing boiler drum composition conditions are not maintained because of the lack of a fresh feed to substitute the evaporated material. For larger time scales, the operation of the BDP must be adjusted to the new composition conditions. These slow dynamics generate a process trajectory that can be seen as the product of integrating material balance, induced by the nth-order integrator s^{-n}, along the distillation process operation.

A feedback controller should be aimed to regulate the BDP operation along the process period. This means that a feedback controller should focus on moderate and large time-scale dynamics of the process. In other words, what is important for feedback control design is the dominant slow dynamics of the process. Because the integrating dynamics dominate over the faster stable ones, a simplified input/output model for a BDP is $G(s) = K_{uy}s^{-n}$. It is clear that, in the time domain, $n = 1$ corresponds to a ramp, $n = 2$ corresponds to a second-order polynomial trajectory and so on. As a first approach, in this work we will consider the simplest case, $n = 1$. From the physical viewpoint, this implies that we are assuming the column conditions (such as the composition in a boiler drum) changes linearly with process time during the operating period. In the time domain, the input/output model can be written as

$$\dot{y} = K_{uy}u \tag{2}$$

where K_{uy} is a (possibly time-varying) high-frequency gain. In this way, the aim of an identification procedure should be to obtain estimates of the single parameter K_{uy}. In principle, this process gain can be obtained as

$$K_{uy} = \frac{\partial \dot{y}}{\partial u} = \frac{d}{dt}\left[\frac{\partial y}{\partial u}\right] \tag{3}$$

That is, K_{uy} is the time derivative of the sensitivity function $\partial y/\partial u$. An open-loop test is proposed for identifying the process gain through the following procedure:

(1) Apply regular relay perturbations $u(t)$ with period P and amplitude Δu around the nominal value u^*.

(2) According to the proposed model in Eq. 2, and because $u(t)$ is discontinuous at $t_d = P/2, P, 3P/2, \ldots$, the output response $y(t)$ is continuous but not differentiable at such time instants. That is, $y(t)$ is only piecewise differentiable. Hence, one can compute the time derivative $\dot{y}(t)$ for all $t \neq t_d$.

(3) At the discontinuity times $t_d = P/2, P, 3P/2, \ldots$, compute the estimated high-frequency gain as

$$K_{uy} = \frac{\dot{y}(t_d^+) - \dot{y}(t_d^-)}{\Delta u} \tag{4}$$

where $\dot{y}(t_d^+)$ and $\dot{y}(t_d^-)$ are, respectively, the time derivatives at $t = t_d$ from the right and the left.

Notice that the effectiveness of the relay procedure relies on the assumption that the response signal is discontinuous at the relay times $t_d = P/2, P, 3P/2, \ldots$. If $y(t)$ is not discontinuous at such time instants, the proposed first-order model in Eq. 2 is not suitable to compute the high-frequency gain. In such a case, higher-order models are required, and the simplest ones are

$$y^{(n)}(t) = K_{uy}u(t)$$

where $y^{(n)}$ denotes the nth-order time derivative of y. That is, the BDP would be described with an n-integrating process. The identification of K_{uy} with these models is more involved because relay perturbations are not sufficient to induce the discontinuous behavior of $y(t)$.

It is expected that, because of the time-varying nature of the BDP, the high-frequency gain K_{uy} be also a time-varying parameter, so that a reliable first-order model of the process should be as follows

$$\dot{y}(t) = K_{uy}(t)u(t) \tag{5}$$

and the time response of the process output is

$$y(t) = y(0) + \int_0^t K_{uy}(\sigma)u(\sigma)d\sigma$$

Notice that, for $u =$ constant, $y(t)$ is given by the integration of the process gain $K_{uy}(t)$. This is because K_{uy} is characterized as high-frequency gain.

Control Design Considerations

Let us consider the case where a distillate composition is the controlled variable, $y = x_D$, and the internal reflux rate r is the manipulated variable u. Note that we will use the internal reflux ratio for computational easiness; however, in practice the manipulated variable is the reflux flow. Nevertheless the procedure presented here for the design of the control law can easily be modified to account this situation. T_m is the temperature at a given tray in the rectifying section. It is assumed that the temperature T_m is measured without delays, and the distillate composition x_D is measured or inferred with delay $\theta > 0$. In this way, x_D and T_m are seen as the primary and the secondary measurement, respectively. It is reasonable to model the input/output responses with the simple models

$$\frac{x_D}{r} = \frac{\tilde{K}_{rx}}{s} \tag{6}$$

and

$$\frac{T_m}{r} = \frac{\tilde{K}_{rT}}{s} \tag{7}$$

where $s = d/dt$ is the Laplace variable, $\tilde{K}_{rx}$ and $\tilde{K}_{rT}$ are constant estimates of the process gains along the operation period. Because x_D is subjected to a measurement delay, the model in Eq. 7 can be completed as follows

$$\frac{x_D}{r} = \frac{\tilde{K}_{rx}\exp(-\theta s)}{s} \tag{8}$$

Equations 7 and 8 become empirical models of the batch distillation dynamics.

The basic control problem is to maintain the distillate composition at a desired trajectory $x_{D,ref}(t)$ by manipulating the internal reflux ratio r. To this end, a feedback controller must be designed on base to the models expressed in Eqs. 7 and 8. Because the temperature measurements are inexpensive and with no time delay, the resulting controller should make use of both composition $\exp(-\theta s)x_D$ and temperature T_m measurements to yield servo responses (set point tracking). Because the primary measurement $\exp(-\theta s)x_D$ is subjected to a large time delay and the secondary measurement T_m is obtained with no delay, it is recommended to use a cascade control structure to achieve the control objectives.

Cascade Control Design

The cascade control configuration consists of two linear controllers arranged in a master/slave structure (see Figure 1): in the master controller, the selected tray temperature T_m is used as a virtual control to regulate the distillate composition x_D and, in the slave controller, the internal reflux rate r is manipulated to drive the tray temperature T_m toward the virtual control signal $T_{m,ref}$. Here, this control design problem will be addressed with a backstepping approach (Krstic et al., 1995). Backstepping methodology offers a natural framework to deal with the cascade structure of the information flow $r(s) \rightarrow T_m(s) \rightarrow x_D(s)$. Given the nonstationary nature of the BDP, the application of traditional cascade control designs suffers from several drawbacks, including the handling of the many secondary measurements. Backstepping methodologies handle in a systematic way the role of primary and secondary measurements in the feedback controller (Giri et al., 1999). As will be shown in later sections, contrary to traditional cascade control

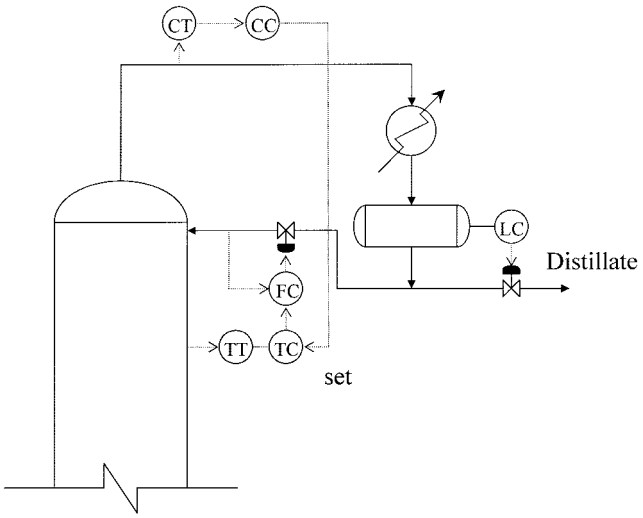

Figure 1. Temperature cascade control configuration to regulate the distillate composition in a batch distillation column.

designs, cascade control design based on backstepping procedures can be extended in a natural way to the case of more than one slave feedback controllers.

The cascade control design can be made following a sequential procedure by first addressing the control design for the "input/output" map $T_m(s) \rightarrow x_D(s)$. In this step, the idea is to obtain a feedback-based design of the required temperature trajectory $T_m(t)$ to achieve composition regulation. In a second step, a feedback function for the actual control input $r(s)$ is designed to guarantee (asymptotic) realization of the required temperature trajectory. The final result is a modular feedback controller that efficiently exploits secondary (temperature) measurements by incorporating them into the control loop as secondary feedback controllers. Besides, tuning can be made easily by independently adjusting the parameters of each feedback control module. In the case of the BDP, the primary feedback loop (master controller) displays slow control actions to avoid instabilities induced by composition time delay. The secondary loop is tuned to give fast control actions to achieve fast temperature tracking. In this way, the resulting cascade controller offers fast protection against disturbances induced by the nonstationary dynamics (that is, changing compositions in the reboiler drum) of the batch distillation operation.

Master controller design

The master controller uses the measured temperature T_m as a virtual control input to control the distillate composition x_D. The idea of the backstepping design is to compute the required temperature trajectory $T_m(t)$ to regulate the distillate composition about a desired trajectory $x_{D,ref}(t)$. This is made by means of a feedback function that plays the role of an inversion operation. It is noted that $x_{D,ref}(t)$ is commonly computed by means of involved inversion, sometimes based on optimization, procedures. In the following, a feedback control function to obtain the required temperature trajectory will be described.

The input/output response from the measured temperature T_m to the distillate composition x_D can be obtained from Eqs. 7 and 8

$$\frac{x_D}{T_m} = \tilde{K}_{Tx}\exp(-\theta s) \tag{9}$$

where $\tilde{K}_{Tx} = \tilde{K}_{rx}/\tilde{K}_{rT}$. In Eq. 9, let us take the temperature T_m as a virtual control input $T_{m,ref}$:

$$\frac{x_D}{T_{m,ref}} = \tilde{K}_{Tx}\exp(-\theta s)$$

The *master control problem* is to design a feedback function $T_{m,ref} = \mu(x_D)$ so that the corresponding closed-loop system is stable and $x_D(t) \rightarrow x_{D,ref}$ asymptotically. The input/output path $\Delta T_{m,ref} \rightarrow \Delta x_D$ displays stable dynamics with a relatively large time delay that limits the maximum achievable bandwidth. Some work has been made to address the problem of robust control design for stable plants with time delays. For instance, Bonnet et al. (2000) provided a parameterization of all stabilizing controllers. Basically, such stabilizing controllers are of the low-gain type with dynamic compensation to improve the response of the primary loop. Based on this idea, a low-gain pure integral controller is sufficient to yield regulation of the system output about the desired set point value $x_{D,ref}$. In this way, the proposed master controller can be given as

$$T_{m,ref}(t) = \tilde{T}_m + \tilde{K}_{Tx}^{-1}\tau_{M,I}^{-1}\int_0^t [x_{D,ref}(\sigma) - x_{D,m}(\sigma)]d\sigma \tag{10}$$

where $\tau_{M,I} > 0$ is the master integral time-constant and $x_{D,m}$ is the measured distillate composition [that is, $x_{D,m} = \exp(-\theta s)x_D$].

Slave controller design

The master feedback control function (Eq. 10) provides a temperature trajectory to ensure distillate composition control. However, the temperature cannot be manipulated by the operators. In fact, the actual manipulated (exogenous) input is the recycling rate r. Following backstepping ideas, the next step is to design a feedback controller in the transfer path $r \rightarrow T_m$ aimed to track the required temperature trajectory $T_{m,ref}(t)$ provided by the master controller. In this way, in the event that $T_m(t) \rightarrow T_{m,ref}(t)$, one can expect that $x_D(t) \rightarrow x_{D,ref}(t)$. Hence, the task for the slave control design is to obtain a feedback compensator that manipulates the internal reflux rate r such that the tray temperature tracks the reference signal $T_{m,ref}(t)$ generated by the master controller.

To design the slave controller, we will follow a modeling error compensation approach as reported by Alvarez-Ramirez et al. (2002). Equation 7 is just an approximated model of the input/output path $r \rightarrow T_m$. Let $\eta[T_m(t), r(t)]$ be the modeling error signal associated with the input/output path $r \rightarrow T_m$. That is, $\eta[T_m(t), r(t)]$ is the signal that matches the actual output signal T_m to that signal produced by the model in Eq. 7. In this way, we can write (see, for instance, Monroy-Loperena and Alvarez-Ramirez, 2001)

$$\dot{T}_m = \tilde{K}_{rT} r + \eta \tag{11}$$

where $\dot{T}_m$ stands for dT_m/dt. The slave controller design is posed as a signal tracking problem where the output of the master controller $T_{m,ref}$ is the signal to be tracked.

If $\xi_m = T_m - T_{m,ref}$ is the tracking error, from Eq. 11 and the fact that (see Eq. 10)

$$T_{m,ref} = \alpha_m(x_D) \overset{def}{=} \tilde{K}_{Tx}^{-1} \tau_{M,I}^{-1}(x_{D,ref} - x_{D,m})$$

we have that

$$\dot{\xi}_m = \tilde{K}_{rT} r + \eta - \alpha_m(x_D) \tag{12}$$

Let us require the slave controller to track the reference signal $T_{m,ref}(t)$ generated by the master controller, with the following dynamics

$$\dot{\xi}_m = -\tau_{S,c}^{-1} \xi_m \tag{13}$$

From Eqs. 12 and 13 we get the *ideal* input/output linearizing feedback control

$$r^{id} = \varphi_S^{id}(x_{D,m}, T_m, \eta) \overset{def}{=} \tilde{K}_{rT}^{-1}[\alpha_m(x_D) - \tau_{S,c}^{-1} \xi_m - \eta] \tag{14}$$

where $\tilde{K}_{rT}^{-1}$ is the process high-frequency gain. The implementation of the feedback control (Eq. 14) relies on an exact cancellation of the modeling error $\eta(t)$. Of course, such implementation is not possible because $\eta(t)$ is unknown. To overcome this situation, the idea is to use an estimate, say $\tilde{\eta}(t)$, of the modeling error instead of the actual one $\eta(t)$ (η replaced by its estimate $\tilde{\eta}$ in Eq. 14). One obtains the following computed slave controller

$$r^c = \varphi_S(x_{D,m}, T_m, \tilde{\eta}) \overset{def}{=} \tilde{K}_{rT}^{-1}[\alpha_m(x_D) - \tau_{S,c}^{-1} \xi_m - \tilde{\eta}] \tag{15}$$

To meet the physical constraint $r \in [r_{\min}, r_{\max}]$, the actual control input r is computed by a saturation function

$$r = \mathrm{Sat}(r^c; r_{\min}, r_{\max}) \overset{def}{=} \begin{cases} r_{\min} & \text{if } r^c \le r_{\min} \\ r^c & \text{if } r_{\min} < r^c < r_{\max} \\ r_{\max} & \text{if } r^c \ge r_{\max} \end{cases} \tag{16}$$

To obtain the estimate $\tilde{\eta}(t)$, advantage is taken from the property that the modeling error signal $\eta(t)$ is strongly observable (Diop and Fliess, 1991) from the measurement T_m. That is, the signal $\eta(t)$ can be reconstructed from temperature measurements in the following way

$$\eta(t) = \dot{T}_m - \tilde{K}_{rT} r \qquad \forall \ t \ge 0 \tag{17}$$

A common practical approach to estimate an observable signal is by means of asymptotic observer schemes (Krstic et al., 1995). In this work, the following reduced-order observer-based estimator is proposed

$$\dot{\tilde{\eta}} = \tau_{S,e}^{-1}[\dot{T}_m - \tilde{K}_{rT} r - \tilde{\eta}] \tag{18}$$

where $\tau_{S,e} > 0$ is an estimation time constant. To avoid the use of a differentiation on T_m, introduce the variable $w = \tau_{S,e}\tilde{\eta} - T_m$, so that the observer (Eq. 18) can be implemented in the following equivalent form

$$\dot{w} = -\tilde{K}_{rT} r - \tilde{\eta} \qquad \tilde{\eta} = \tau_{S,e}^{-1}(w + T_m) \tag{19}$$

with initial condition $w(0) = -T_m(0)$. In combination of this observer with the controller (Eq. 15), Eq. 16 yields our candidate slave measurement driven controller

$$\dot{w} = -\tilde{K}_{rT} r - \tau_{S,e}^{-1}(w + T_m) \qquad r^c = \varphi_S(x_{D,m}, T_m, \tilde{\eta})$$
$$r = \mathrm{Sat}(r^c; r_{\min}, r_{\max}) \tag{20}$$

Summarizing, the application of a backstepping procedure together with a modeling error estimator led us to a candidate cascade control configuration to control the distillate composition. The proposed master/slave feedback controller is equivalent to a parallel cascade controller with low-gain composition feedback and high-gain temperature feedback. This control configuration presents the following features:

(1) The master controller (outer slow loop) provides the tray reference temperature to the slave (inner fast loop) controller.

(2) The uncertainty η of the input/output $r \to T_m$ path is quickly estimated and compensated in the slave loop, and uncertainties and time delay related to the input/output $T_m \to x_D$ path are compensated in the master loop by pure integral action.

(3) The scheme in Eq. 10, with Eq. 20 arising from a master/slave design, uses the output of the master controller $T_{m,ref}$ to compute the tracking error $\xi_m(t) = T_m - T_{m,ref}$.

(4) If the modeling error signal $\eta(t)$ is estimated and cancelled very quickly by choosing a sufficiently small estimation parameter $\tau_e > 0$, then $T_m(t)$ will converge quickly to $T_{m,ref}(t)$. In this way, the performance induced by the master controller will be achieved as $T_m(t) \to T_{m,ref}(t)$. This leads to the conclusion that the overall performance is strongly limited by the master controller action.

Table 1. Case Study Configuration

Specifications	
System	Cyclohexane (1) *n*-Heptane (2) Toluene (3)
Thermodynamic model	Ideal
Pressure, kPa	101.3
Reboiler heat flow rate, kW	15
Tray holdup, mol	2.0
Reflux drum holdup, mol	35.0
Total feed charge, mol	3000.0
Nominal feed composition (mole fraction)	0.40/0.40/0.20
Tray hydraulic time constant, h	0.001
Number of ideal trays, including condenser and reboiler	30
Cyclohexane nominal composition setpoint	0.95

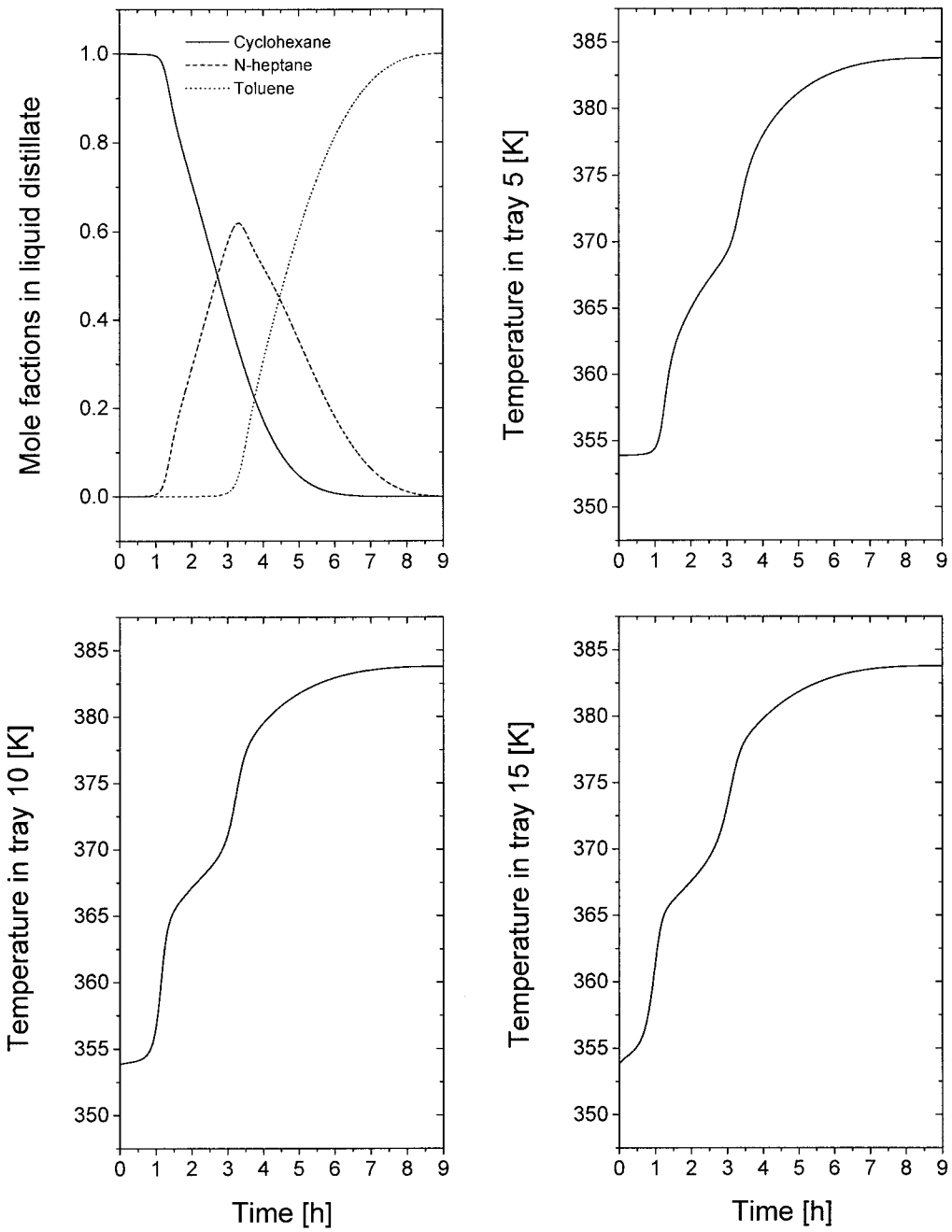

Figure 2. Dynamics of the *uncontrolled* distillate composition and temperatures at trays 5, 10, and 15.

Tuning Guidelines

The control design described above suggests the following guidelines on tuning:

(1) In a first step, choose the integral time constant $\tau_{M,I} > 0$ so as to obtain closed-loop stability in the input/output $T_m \rightarrow x_D$ path. Following IMC ideas (Morari and Zafiriou, 1989), choose a value of $\tau_{M,I}$ that is not smaller than the underlying time delay $\theta \geq 0$.

(2) Set the values of the closed-loop time constants, $\tau_{S,c} > 0$, of the order of 0.025 the operation period.

(3) The parameter $\tau_{S,e} > 0$ defines the rate of convergence of the estimation error. Because the slave (inner) loop is designed to track the temperature reference trajectory provided by the master (outer) loop, the slave loop should be faster than the master loop. In principle, the slave estimation time constant $\tau_{S,e}$ should be chosen about 3 to 10 times smaller than the nominal closed-loop time constant $\tau_{S,c} > 0$. The rationale behind this recommendation is to estimate modeling error signals faster than the expected response time constant of the process.

These tuning recommendations resemble well-accepted industrial practices. Moreover, the tuning of the cascade linear controller structure is particularly easy to carry out in view of the fact that, up to the point where the influence of unmodeled

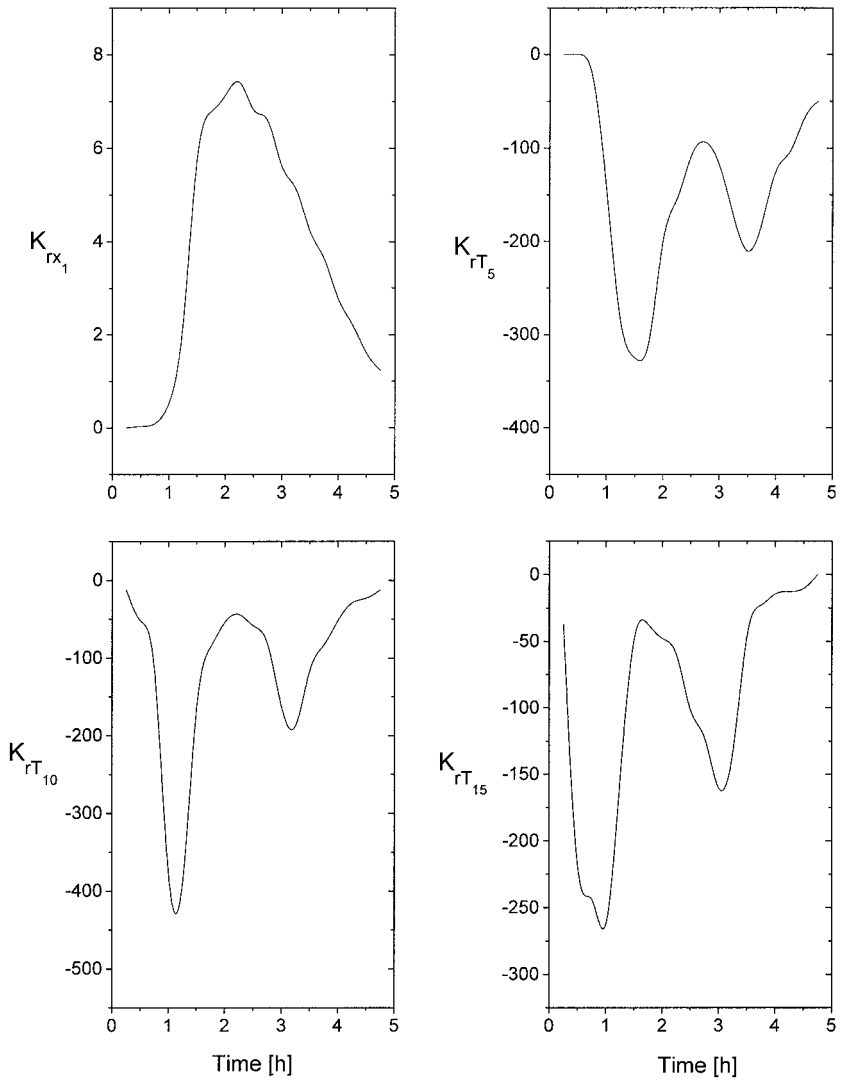

Figure 3. Time-variant gains between: the internal reflux ratio and the distillate composition of component one (cyclohexane), K_{rx_1}, internal reflux ratio and temperature in tray 5, K_{rT_5}, internal reflux ratio and temperature in tray 10, $K_{rT_{10}}$, and internal reflux ratio and temperature in tray 15, $K_{rT_{15}}$.

dynamics and measurement noise is no longer negligible, the robustness of the closed-loop system increases monotonically with $\tau_{S,e}^{-1}$.

Extension to Multiple Temperature Measurements

The addition of a tray temperature as a secondary measurement enhances the capabilities of distillate composition control. Because temperature measurements are fast and inexpensive, it is reliable to add more than one temperature measurements. By measuring temperature at several trays a fast feedforward action can be obtained. The systematic procedure described before can be easily extended to the control design with multiple temperature measurements.

A brief outline of cascade composition control with multiple temperature measurements is given as follows. Let $(T_{m,1}, T_{m,2}, \ldots, T_{m,p})^T \in \mathbb{R}^p$ be a set of ordered measured temperatures with respect to the top tray. As before, consider the one time-constant model

$$\frac{x_D}{r} = \frac{\tilde{K}_{rx}\exp(-\theta s)}{s} \tag{21}$$

and

$$\frac{T_{m,j}}{r} = \frac{\tilde{K}_{rT_j}}{s} \qquad j = 1, \ldots, p \tag{22}$$

where $\tilde{K}_{rx}$ and $\tilde{K}_{fT_j}$ are constant estimates of the process gains along the operation period; and r, x_D, and T_m are the internal reflux rate, distillate composition, and measured tray temperatures, respectively. The idea for multiple temperature cascade control is as follows:

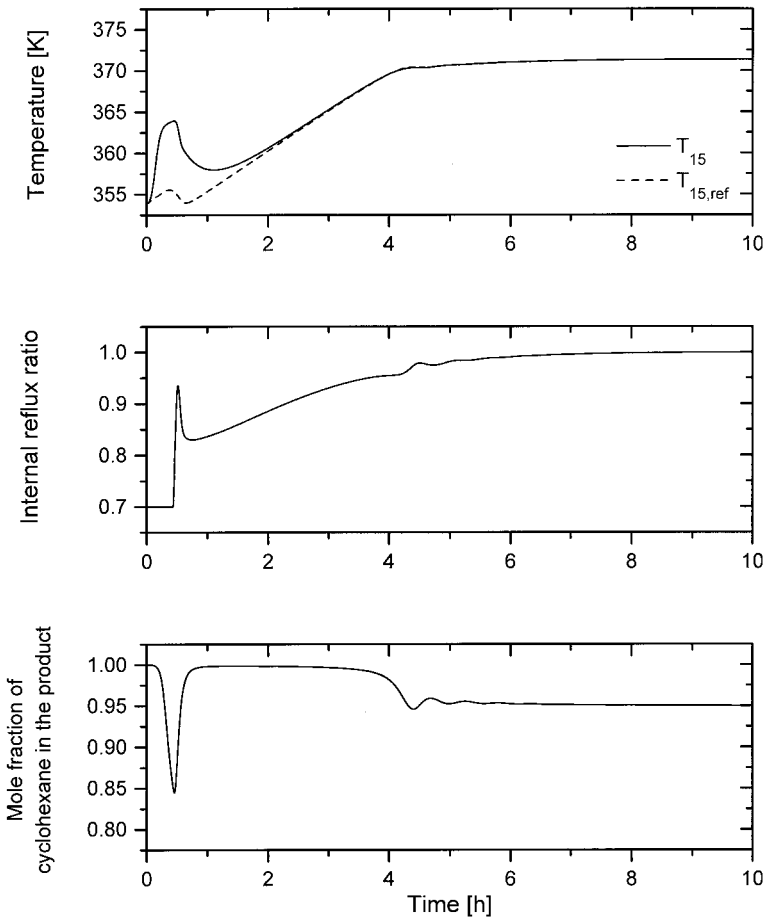

Figure 4. Time evolution of the batch distillation process with master/1-slave controller for a product purity of $x_{1,D,ref} = 0.95$, with constant process gains estimates as the mean of the time-varying high-frequency gains.

• *Step 1.* Use $T_{m,1}$ as a virtual control input to control the distillate composition x_D. This provides the set point trajectory $T_{m,1,ref}$ for the first slave loop.

• *Step j.* Use $T_{m,j}$ as a virtual control input to control the tray temperature $T_{m,j-1}$ along the trajectory $T_{m,j-1,ref}$. This provides the set point trajectory $T_{m,j-1,ref}$ to the jth slave loop.

• *Step p + 1.* Use r to control the tray temperature $T_{m,p}$ along the trajectory $T_{m,p,ref}$.

The final product is a cascade controller in master/p-slave configuration, where the p-slave controller is a series of p temperature controllers ordered in cascade form. Notice that this procedure reduces to a single master/slave controller when $p = 1$.

Having built the master controller to regulate the distillate composition by manipulating the trajectory $T_{m,1,ref}$ of the first measured tray temperature, the task for the jth slave control design is to obtain a controller that manipulates the trajectory $T_{m,j+1,ref}$ such that the tray temperature tracks the reference signal $T_{m,j,ref}(t)$ generated by the $(j-1)$th slave controller. By taking $\eta[T_{m,j}(t), T_{m,j+1}(t)]$, the modeling error associated with the input/output path $T_{m,j} \rightarrow T_{m,j+1}$, the construction of the jth slave temperature controller is similar to that described in an earlier subsection (Slave controller design). All the slave controllers have a linear control structure with $T_{m,j} - T_{m,j,ref}$ being the corresponding jth tracking error. Besides, the p-slave construction allows the introduction of control saturations at all levels, thus taking $T^{\min}_{m,j,ref}$ and $T^{\max}_{m,j,ref}$ the minimum and maximum jth reference values, respectively. This nested saturations reduces under- and overshooting induced by high-gain estimations.

It should be recognized that, although the use of several temperature measurements can be effective, in this case the control system is more prone to sensor failure. In fact, because the control law is arranged in a series configuration, the failure of a temperature sensor will inactivate the feedback control action of *downstream* loops.

Numerical Simulations

A rigorous nonlinear model of the BDC, with parameters given in Table 1, was used to illustrate the control design and its performance. The differential equations arising from energy and material balances were simultaneously solved by means of an implicit Euler approximation with a time step equal to 0.01 h. At each time step, the resulting nonlinear algebraical equations were solved by means of a Newton–Raphson method endowed with a sparse matrix solver to exploit the sparsity of the incidence Jacobian matrix. Because the trajectories of the BDC are continuous in time, the Newton–Raphson method was implemented as a continuation method where the state of the

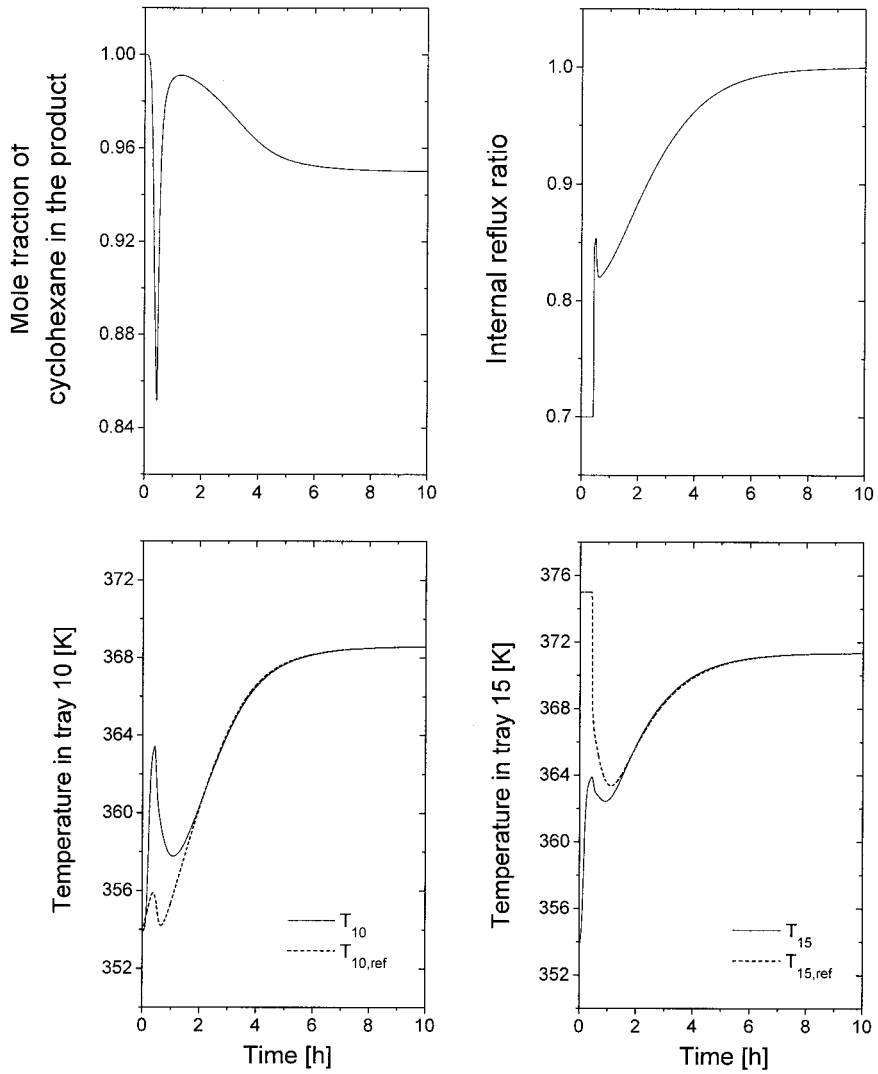

Figure 5. Time evolution of the batch distillation process with master/2-slave controller for a product purity of $x_{1,D,ref} = 0.95$, with constant process gains estimates as the mean of the time-varying high-frequency gains.

preceding time step was taken as an initial guess for the actual step. In this way, the Newton–Raphson required two or three iterations to achieve a relative error $< 2\%$. The numerical procedure was implemented as a FORTRAN program in a PC-Pentium IV computer.

In all simulations, the production step or steps are presented, given that the startup period objective is to leave the column at total reflux conditions, and this is done in an open-loop fashion. Figure 2 presents the time evolution of the *uncontrolled* overhead product composition for a fixed external reflux, L_1/D, equal to 4.0 (internal reflux ratio r, equal to 0.8). The rationale behind the selection of $r = 0.8$ is that most time the column will operate at such condition. However, for a more reliable process identification, several values of r should be tried. This case is taken as the nominal case to apply the identification procedure described previously. After the application of the identification procedure with period $P = 0.5$ h and amplitude 5% on the internal reflux ratio (r^*), the time-varying process gains between: the internal reflux ratio and the distillate composition of component one (cyclohexane), K_{rx_1}; internal reflux ratio and temperature in tray 5, K_{rT_5}; internal reflux ratio and temperature in tray 10, $K_{rT_{10}}$; and internal reflux ratio and temperature in tray 15, $K_{rT_{15}}$, are presented in Figure 3. Notice the time-varying nature of the process gains K_{rx_1}, K_{rT_5}, $K_{rT_{10}}$, and $K_{rT_{15}}$. As the operation time advances, K_{rx_1} achieves a maximum value and then decreases to achieve a steady-state value as the cyclohexane is exhausted (see Figure 2). Of course, this steady-state value is meaningless because at this time the batch distillation process, to recover the cyclohexane, has ended. On the other hand, the process gains K_{rT_5}, $K_{rT_{10}}$, and $K_{rT_{15}}$ present two minimum values caused by the inflection in composition of n-heptane near 3.5 h. From the physical viewpoint, such minima could be attributed to the traveling of temperature waves from the bottom to the top of the column (see Figure 2). Such traveling waves reflect composition transitions into the column, which are observed as inflections in the output composition dynamics. In this way, a minimum value in the process gain gives transition-form operating conditions, which are recast in the process gain value. Also notice that

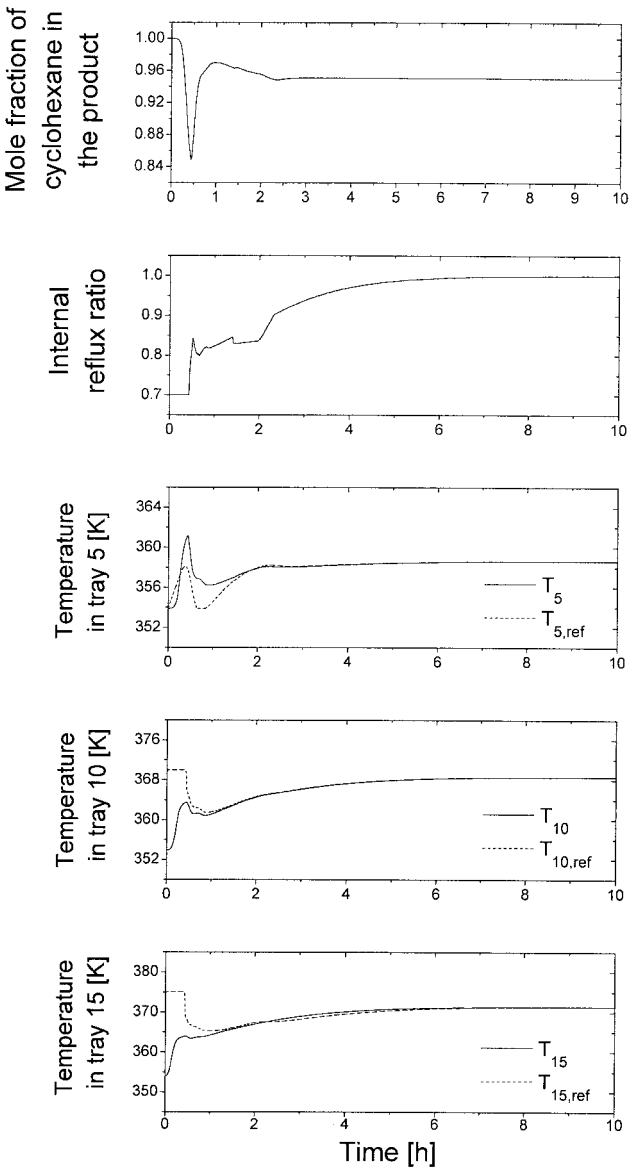

Figure 6. Time evolution of the batch distillation process with master/3-slave controller for a product purity of $x_{1,D,ref} = 0.95$, with constant process gains estimates as the mean of the time-varying high-frequency gains.

the temperature gains do not reach a steady state, given that the BDP has not finished.

Consider the following conditions and parameters to be used in the proposed multicascade control scheme to regulate the distillate composition:

(1) The regulation task will consist in tracking a constant composition trajectory of component one (cyclohexane) in the distillate, $x_{1,D,ref} = 0.95$.

(2) A time-delay $\theta = 0.083$ h is considered because typical measurement times in chromatography equipment for this kind of mixture is of the order of 0.10 h.

(3) Following the tuning guidelines described previously, the following master and slave control parameters were used: $\tau_{M,I} = 0.15$ h, $\tau_{S,c,j} = 0.30$ h, and $\tau_{S,e,j} = 0.10$ h.

With this set of control parameters, the following set of numerical simulations test were carried out.

Effect of Gain Estimation. Three multicascade control configurations are considered in this subsection: (1) a master/1-slave configuration with tray 15 used to locate the secondary temperature measurement; (2) for master/2-slave configuration, trays 15 and 10 are used to locate the secondary temperature measurements; and (3) a master/3-slave configuration with trays 15, 10, and 5 are used to locate the secondary temperature measurements. First, consider that the process gains are constant estimates, taken as the mean of the estimated (time-varying) high-frequency gain

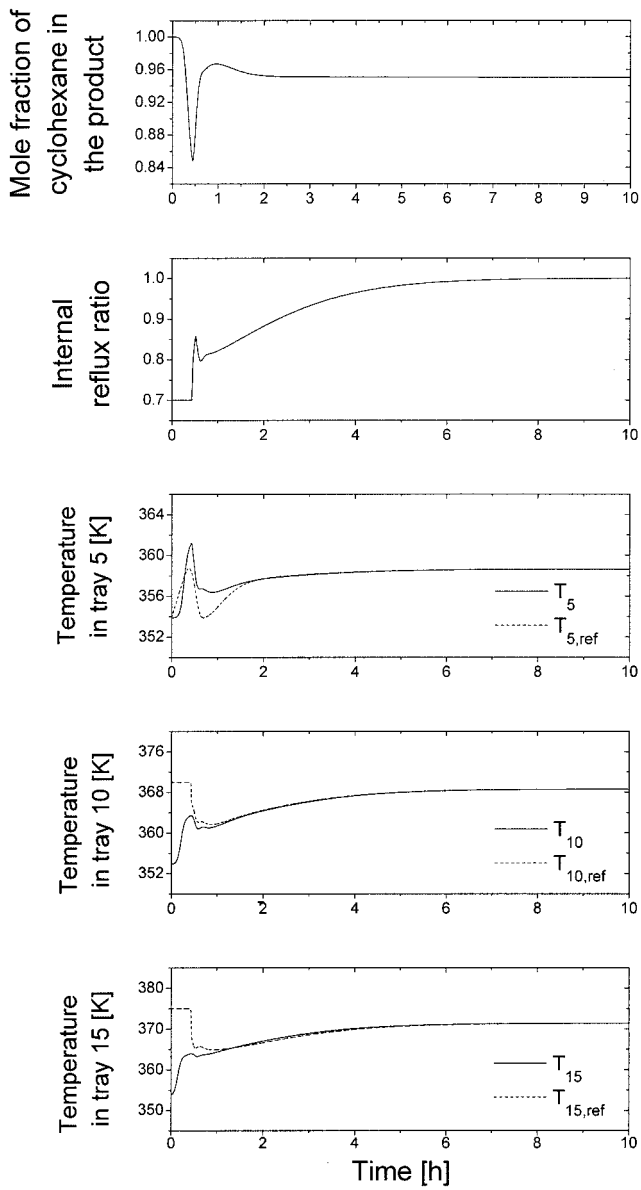

Figure 7. Time evolution of the batch distillation process with master/3-slave controller for a product purity of $x_{1,D,ref} = 0.95$, with constant process gains estimates as the highest magnitude of the time-varying high-frequency gains.

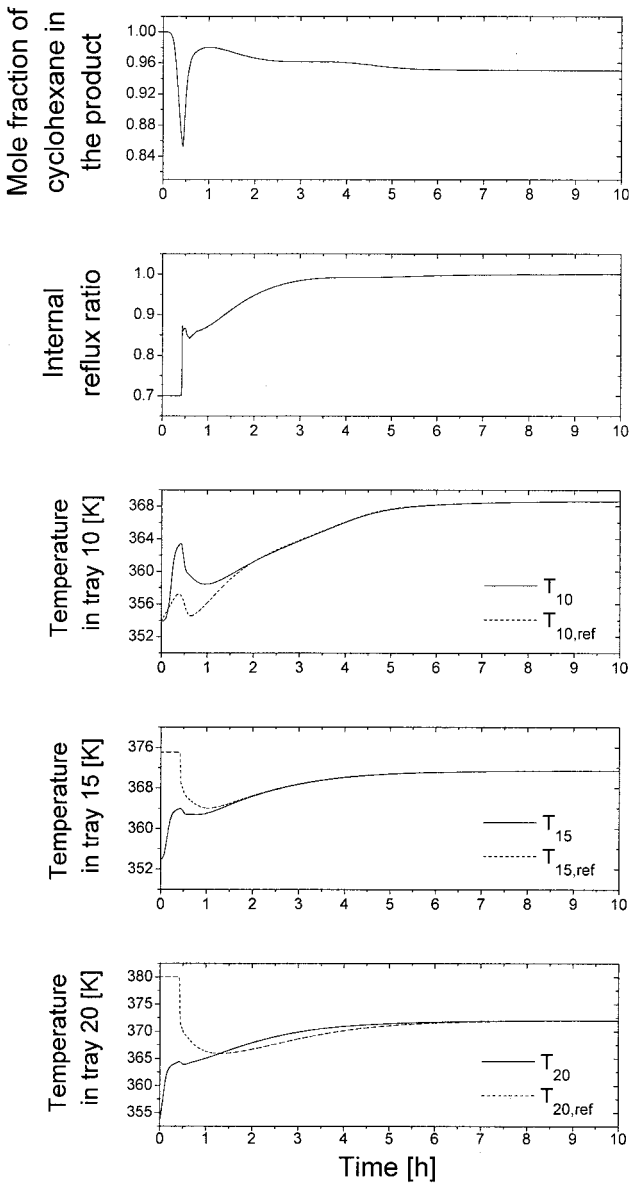

Figure 8. Time evolution of the batch distillation process with master/3-slave controller when the temperature measurements are in trays 10, 15, and 20.

$$\tilde{K}_{uy} = \frac{1}{t_f}\int_0^{t_f} K_{uy}(\sigma)d\sigma$$

According to the models expressed in Eqs. 6 and 7, the plant parameters are: $\tilde{K}_{rx_1} = 3.64\ \text{h}^{-1}$, $\tilde{K}_{rT_5} = -29.36\ \text{K h}^{-1}$, $\tilde{K}_{rT_{10}} = -23.27\ \text{K h}^{-1}$, and $\tilde{K}_{rT_{15}} = -19.46\ \text{K h}^{-1}$. Figure 4 shows the time evolution for the master/1-slave configuration. Note that the controller presents a pronounced overshoot in the first 3 h of the process, driving the overhead composition close to unity. After these 3 h the control scheme quickly drives the composition to the set point trajectory, until the reference temperature reaches the tray temperature at tray 15. Nevertheless the behavior of the internal reflux ratio is smooth and monotonic. The master/2-slave configuration behavior is presented in Figure 5. Compared with master/1-slave, the overshoot was decreased and a faster drive of the controller to the set point trajectory is noticed. Also note that the reference temperatures at trays 15 and 10 are basically the same as the actual temperatures at the respectively trays after 2 h of operation. In this case the behavior of the internal reflux ratio is smooth and monotonic as in the master/1-slave case. Now consider the time evolution for the master/3-slave configuration, shown in Figure 6. This case presents the smallest overshoot of the three configurations studied. Note that the reference temperatures at trays 5, 10, and 15 reach the tray temperatures in 2 h, but in this case the behavior of the reflux rate is monotonic but not smooth, occurring because the control

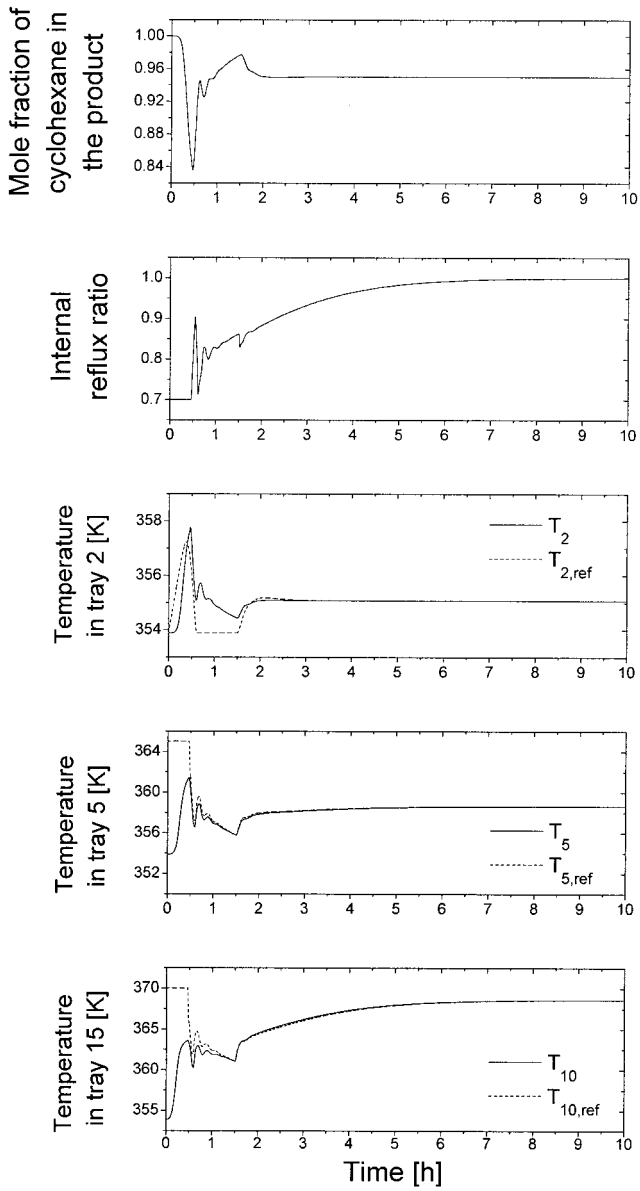

Figure 9. Time evolution of the batch distillation process with master/3-slave controller when the temperature measurements are in trays 2, 5, and 10.

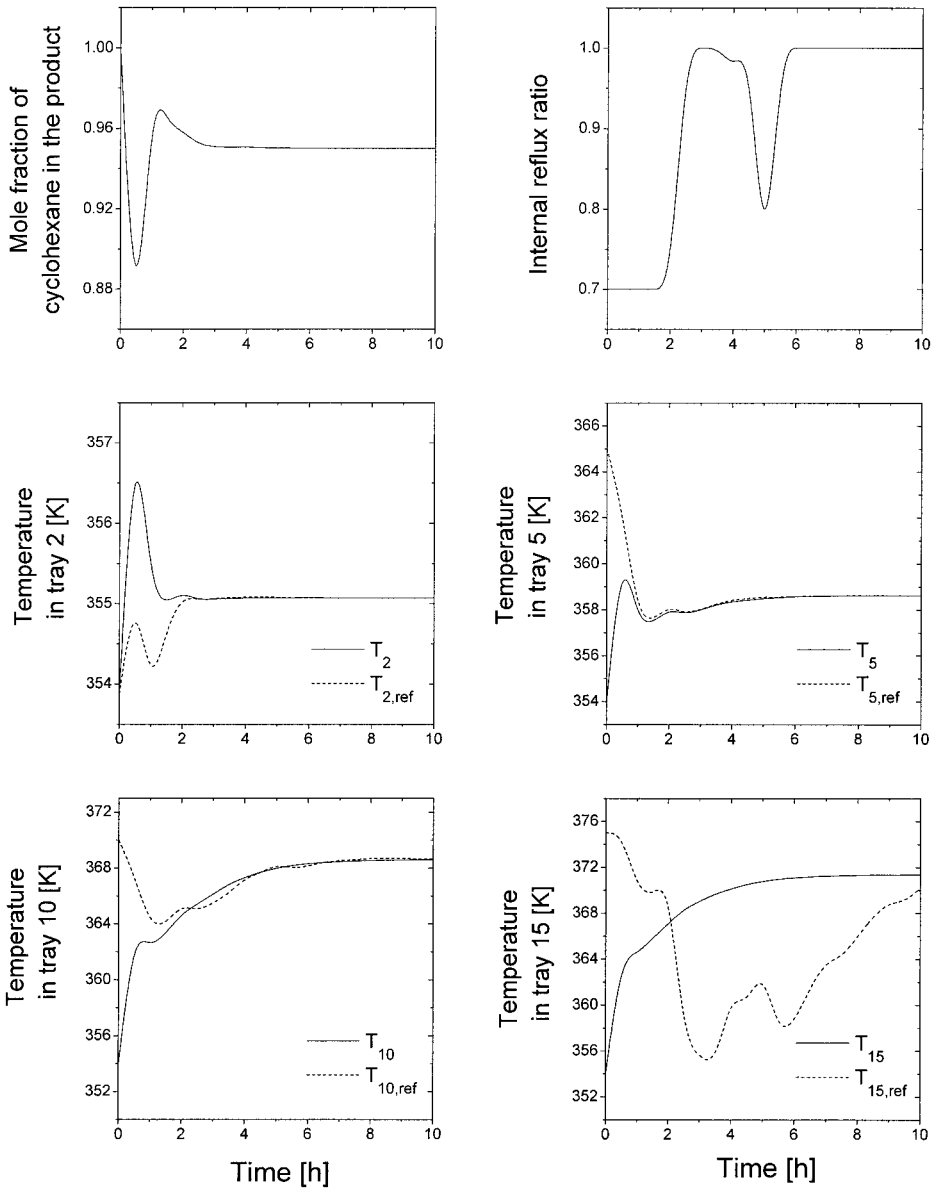

Figure 10. Time evolution of the batch distillation process with master/4-slave controller when the temperature measurements are in trays 2, 5, 15, and 20.

configuration tends to reach the reference trajectory as quickly as the delay of the BDP allows. To show the performance of the controller with another estimation of the high-frequency gains, consider them as the highest magnitude of the time-varying high-frequency gains, as

$$\tilde{K}_{uy} = \text{sgn}(K_{uy})\max(|K_{uy}|)$$

for which assumption the plant parameters are: $\tilde{K}_{rx_1} = 7.40$ h^{-1}, $\tilde{K}_{rT_5} = -325.00$ K h^{-1}, $\tilde{K}_{rT_{10}} = -425.00$ K h^{-1}, and $\tilde{K}_{rT_{15}} = -265.00$ K h^{-1}. As expected with this kind of estimates the controllers will be faster. Figure 7 shows the time evolution for a master/3-slave configuration. Basically the shapes of Figure 7 are the same as those in Figure 6, but note that the overshoot is lower and the controller drives the composition trajectory to the reference trajectory faster. This observation is important because one can observe that the greater magnitude of the high-frequency gains between the internal reflux ratio and the temperatures assist the servo configuration. Similar results are found for the master/1-slave and master/2-slave configurations. These results suggest that a gain scheduling will improve the controller performance. This issue is under study and will be reported elsewhere.

Effect of Temperature Measurement Location. Figure 8 shows the time evolution for a master/3-slave configuration when trays 10, 15, and 20 are used to locate the secondary temperature measurements. For this case the high-frequency gains are considered as the mean of the estimated (time-varying) high-frequency gains, being $\tilde{K}_{rT_{20}} = -21.75$ K h^{-1}. Compared to the behavior of Figure 6, the configuration of Figure 8 is slower because the set point is reached after 5 h of the operation time. Figure 9 shows the time evolution for a

master/3-slave configuration when trays 2, 5, and 10 are used to locate the secondary temperature measurements. As in the preceding case the high-frequency gains are considered as the mean of the estimated (time-varying) high-frequency gains, being $\tilde{K}_{rT_2} = -23.20$ K h^{-1}. With respect to the behavior of Figure 6, the configuration of Figure 9 is faster because the set point is reached in less than 2 h of the operation time. Similar results are obtained for the master/1-slave and master/2-slave configurations. For this BDP, it is noted that the closer the temperature measurement to the top of the column, the better the controller performance. However, the problem is that the closer the temperature measurement to the top of the column, the lower the sensitivity of temperature to changes in compositions, and the larger the impact of temperature noise. Of course, this situation imposes a limitation in the temperature measurement location, and hence in the control performance.

Number of Temperature Measurements. Now consider the case where a master/4-slave configuration when trays 2, 5, 10, and 15 are used to locate the secondary temperature measurements. For this case the high-frequency gains are considered as the mean of the estimated (time-varying) high-frequency gains. Figure 10 shows the time evolution for this configuration. Note that the reference temperature at tray 15 drives very slowly to the tray temperature, and the behavior of the internal reflux ratio first stays at its lower saturation value in the first 2 h, then goes quickly to the total reflux and begins to decrease for 2.5 h and then increases again to the total reflux value. Thus the behavior of the internal reflux ratio is very different with respect to all the cases studied. However, the control goal is reached after 2 h. These results suggest the existence of an optimal number of slaves in a multicascade scheme. This issue is under study and will be reported elsewhere.

Measurement Noise. Consider the case where temperature measurements were contaminated with a zero-mean and 2 K standard deviation, and composition measurements were contaminated with a zero-mean and 0.005 standard deviation. In both cases a Gaussian noise was generated with a standard random number generator. According to Figure 11 for a master/3-slave configuration, the cascade controller is able to provide acceptable performance without excessive amplification of the measurement noise.

Multiple Separation. To show the performance of the proposed multicascade controller in a more real situation, consider the separation of the two most volatile components. The objective of the separation is to recover the more volatile component and the intermediate component at a constant purity. In industrial practice, the column is started up as usual, then the more volatile component is withdrawn at the required constant purity until the internal reflux ratio reaches a specified maximum value. At this point, the reflux rate is lowered (that is, following a ramp decrement) to allow the intermediate component to reach the top of the column. When this component has reached the desired purity, the constant composition control is started again. Figure 12 shows the time evolution for the recovering of cyclohexane at a constant purity $x_{1,D,ref} = 0.95$, and in the second step *n*-heptane is recovered at a constant purity of $x_{2,D,ref} = 0.95$. For this purpose, the controller parameters for the recovering of cyclohexane are taken as in Figure 7. For the recovering of *n*-heptane the estimated process gains were estimated, but now considering the operation time between 3.75 and 7.5 h, giving $\tilde{K}_{rx_2} = 0.56$ h^{-1}, $\tilde{K}_{rT_5} = -12.84$ K h^{-1}, $\tilde{K}_{rT_{10}} = -4.51$ K h^{-1}, and $\tilde{K}_{rT_{15}} = -1.37$ K h^{-1}. Also $\tau_{M,I}$ is taken as 1.5 h. Figure 12 shows the time evolution for the recovering of the two components. As in the case of the recovering of the lightest component (cyclohexane), the master/3-slave configuration in both steps achieves the desired closed-loop goals.

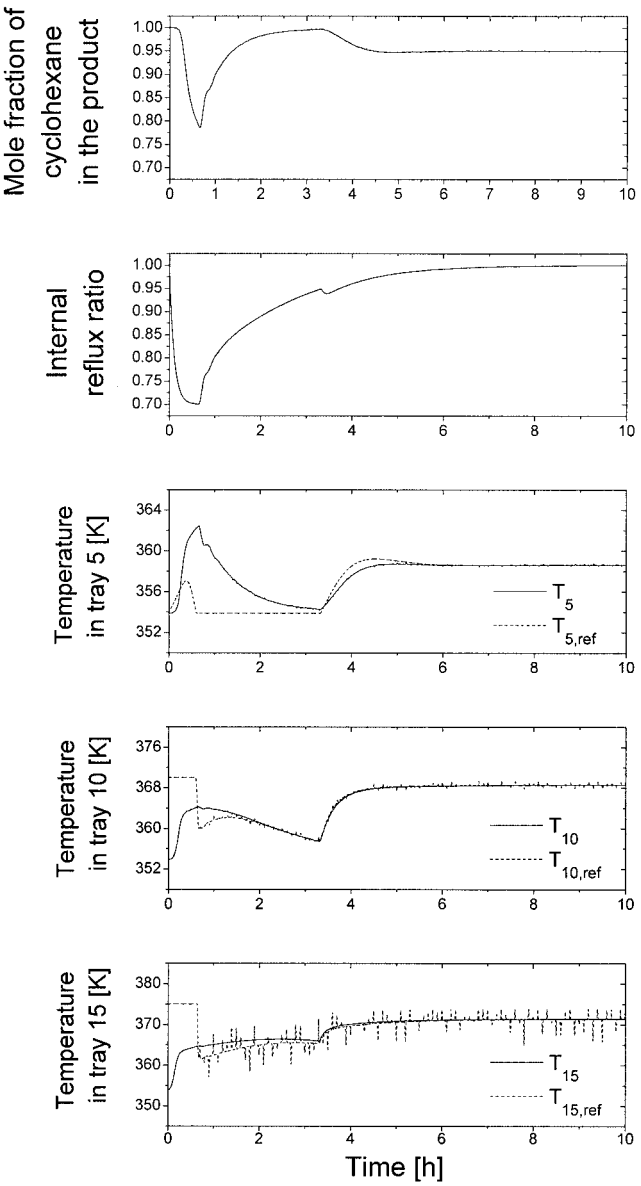

Figure 11. Time evolution of the batch distillation process with master/3-slave controller with a measurement temperature noise of ±2*K* and a measurement composition noise of ±0.005.

Comparison with an Exact Nonlinear Controller. The performance of a master/3-slave controller was compared with the performance of an exact nonlinear inverse-dynamics controller (see Barolo and Berto, 1998). By an exact inverse-dynamics controller we mean that exact knowledge of the process parameters and exact measurements of stage compositions are available. Of course, this is not possible in practice, and the comparison is made only to underscore the performance of the

proposed cascade controller. Figure 13 shows the time evolution of the distillate composition and the reflux flow rate. As expected, it is noted that better performance is obtained with the exact nonlinear controller. However, such improved performance is obtained at the expense of exact process information, including vapor–liquid equilibrium and stage composition measurements. On the other hand, acceptable closed-loop performance is obtained with a cascade control structure with an inexpensive implementation, relying on only one composition measurement (the distillation composition) and several standard stage temperature measurements.

Conclusions

In this work, we have addressed the overhead composition control through a multicascade scheme that is constructed following a backstepping approach. Based on an open-loop identification procedure, the proposed multicascade controller has a simple, linear structure that can be easily implemented on standard technologies. The resulting controller presents three advantages: (1) the master composition controller drives the slave temperature controller with information on the temperature set point and its time derivative, (2) the input/output matching term of the slave controller is effectively compensated by a simple reduced-order observer that runs faster than the slave loop dynamics, and (3) opens the possibility of enhancing the controller performance by incorporating more than one temperature measurement in each cascade controller.

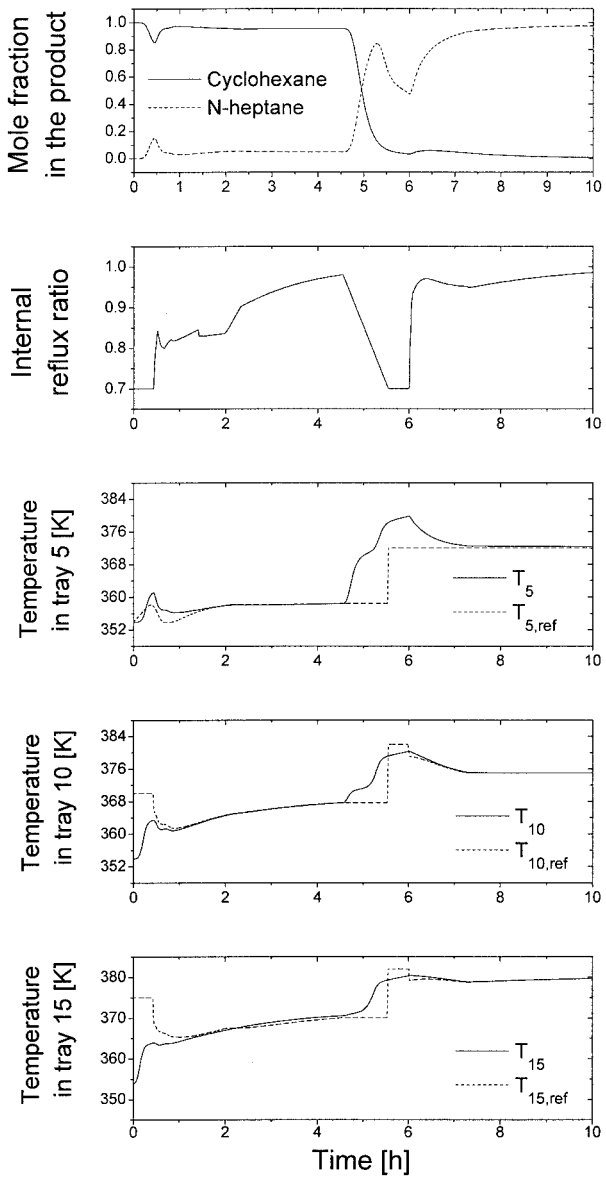

Figure 12. Time evolution of the controlled batch distillation for two product specifications.

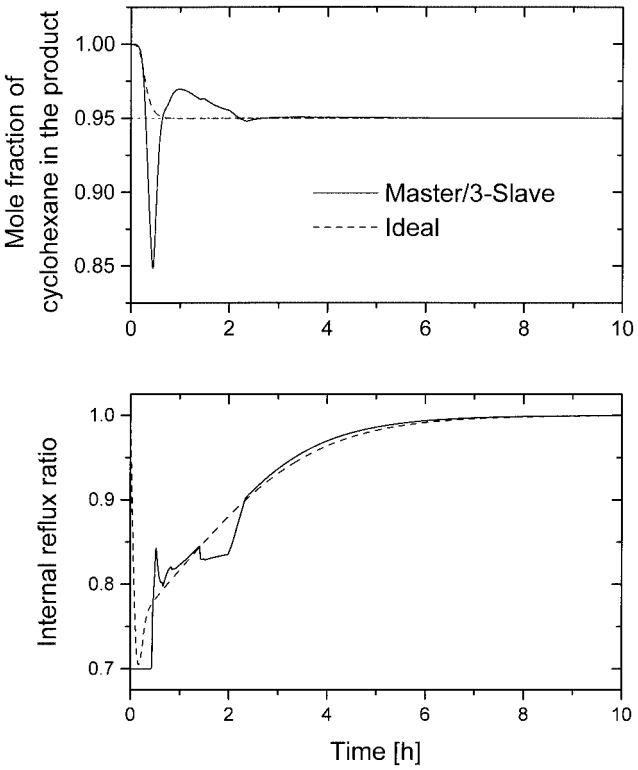

Figure 13. Performance comparison between the exact nonlinear inverse-dynamics controller (see Barolo and Berto, 1998) and master/3-slave controller when the temperature measurements are in trays 2, 5, and 10.

Literature Cited

Alvarez-Ramirez, J., R. Monroy-Loperena, Cervantes, I., and A. Morales, "A Novel Proportional-Integral-Derivative Control Configuration with Application to the Control of Batch Distillation," *Ind. Eng. Chem. Res.*, **39**, 432 (2000).

Barolo, M., and F. Berto, "Composition Control in Batch Distillation: Binary and Multicomponent Mixtures," *Ind. Eng. Chem. Res.*, **37**, 4689 (1998).

Bonnet, C., J. R. Partington, and M. Sorine. "Robust Stabilization of a Delay System with Saturating Actuator or Sensor," *Int J. Robust Nonlinear Contr.*, **10**, 579 (2000).

Bosley, J. R., and T. F. Edgar, "Application of Nonlinear Model Predictive Control to Optimal Batch Distillation," *IFAC Symposia Series*, **2,** 303 (1993).

Dechechi, E. C., L. F. L. Luz Jr., A. J. Assis, M. R. W. Maciel, and R. Maciel-Filho, "Interactive Supervision of Batch Distillation with Advanced Control Capabilities," *Comput. Chem. Eng. Suppl.*, **22**, S867 (1998).

Diop, S., and M. Fliess, "On Nonlinear Observability," Proc. of 1st European Control Conference, Hermés: Hamburg. Germany, Vol. 1, p. 152 (1991).
Diwekar, U. M., *Batch Distillation, Simulation, Design and Control*, Taylor & Francis, London (1995).
Fileti, A. M. F., and J. A. F. Rocha-Pereira, "The Development and Experimental Testing of Two Adaptive Control Strategies for Batch Distillation," *Distillation and Absorption '97*, R. Darton, ed., IChemE: Rugby, UK, p. 249 (1997).
Giri, F., A. Rabeh, and F. Ikhouane, "Backstepping Adaptive Control of Time-Varying Plants," *Syst. Contr. Lett.*, **36**, 245 (1999).
Henson, M. A., and D. E. Seborg, *Nonlinear Process Control*, Prentice-Hall, PTR, London (1997).
Kim, Y. H., "Optimal Design and Operation of Multi-Product Batch Distillation Column Using Dynamic Models," *Chem. Eng. Process.*, **38**, 61 (1999).
Krstic, M., I. Kanallakopoulus, and P. V. Kokotovic, *Nonlinear and Adaptive Control Design*, Wiley, New York (1995).
Li, P., and G. Wozny, "Tracking the Predefined Optimal Policies for Multiple-Fraction Batch Distillation by Using Adaptive Control," *Comp. Chem. Eng.*, **25**, 97 (2001).
Monroy-Loperena, R., and J. Alvarez-Ramirez, "Dual Composition Control in a Middle-Vessel Batch Distillation Column," *Ind. Eng. Chem. Res.*, **40**, 4377 (2001).
Morari, M., and E. Zafiriou, *Robust Process Control*, Prentice-Hall, New York (1989).
Oisiovici, R. M., and S. L. Cruz, "Inferential Control of High-Purity Multicomponent Batch Distillation Columns Using an Extended Kalman Filter," *Ind. Eng. Chem. Res.*, **40**, 2628 (2001).
Quintero-Marmol, E., W. L. Luyben, and C. Georgakis, "Application of an Extended Luenberger Observer to the Control of Multicomponent Batch Distillation," *Ind. Eng. Chem. Res.*, **30**, 1870 (1991).

Appendix: Dynamical Model for Batch Distillation Columns

In this Appendix we consider the governing equations derived from mass and energy balances for a multicomponent batch distillation column, for N_C components, as shown in Figure A1, where tray one is the condenser and tray N is the reboiler. The model is valid under the following assumptions: (1) Liquid on the tray is perfectly mixed and incompressible, (2) the vapor-phase holdup is assumed to be negligible compared to the liquid-phase holdup on each tray, (3) vapor and liquid leaving the tray are in physical equilibrium, (4) the pressure is assumed constant over all the column, and (5) the control of levels in condenser and reboiler is perfect.

Consider the following notation: D is the overhead product flow rate, H is the molar enthalpy in the vapor phase, h is the molar enthalpy in the liquid phase, K is the vapor–liquid equilibrium ratio, L is the molar liquid flow rate, M is the molar holdup, P is the absolute pressure, Q is the heat flow rate, T is the absolute temperature, V is the vapor flow rate, x is the liquid molar fraction, and y is the vapor molar fraction. Also, consider the following subscripts: R for reboiler, C for condenser, i for the ith component, j for the jth tray, and N for the total number of trays.

We have the following dynamical equations.

Condenser

Overall Material Balance

$$\frac{dM_1}{dt} = V_2 - L_1 - D \tag{A1}$$

Component Material Balance

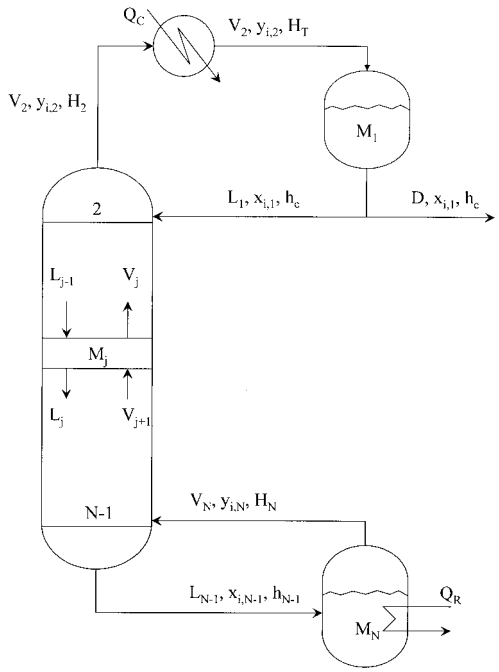

Figure A1. Batch distillation column.

$$\frac{d(M_1 x_{i,1})}{dt} = V_2 y_{i,2} - L_1 x_{i,1} - D x_{i,1} \qquad \forall\ i \in \underset{N_C}{\mathbf{I}} \tag{A2}$$

Energy Balance

$$\frac{d(M_1 h_C)}{dt} = V_2 H_T - L_1 h_C - D h_C \tag{A3}$$

where

$$V_2(H_T - H_2) = Q_C \tag{A4}$$

General trays

Overall Material Balance

$$\frac{dM_j}{dt} = V_{j+1} - V_j + L_{j-1} - L_j \tag{A5}$$

Component Material Balance

$$\frac{d(M_j x_{i,j})}{dt} = V_{j+1} y_{i,j+1} - V_j y_{i,j} + L_{j-1} x_{i,j-1} - L_j x_{i,j} \qquad \forall\ i \in \underset{N_C}{\mathbf{I}} \tag{A6}$$

Energy Balance

$$\frac{d(M_j h_j)}{dt} = V_{j+1} H_{j+1} - V_j H_j + L_{j-1} h_{j-1} - L_j h_j \tag{A7}$$

Reboiler system

Overall Material Balance

$$\frac{dM_N}{dt} = L_{N-1} - V_N \tag{A8}$$

Component Material Balance

$$\frac{d(M_N x_{i,N})}{dt} = L_{N-1}x_{i,N-1} - V_N y_{i,N} \qquad \forall\ i \in \mathbf{I}_{N_C} \tag{A9}$$

Energy Balance

$$\frac{d(M_N h_N)}{dt} = L_{N-1}h_{N-1} - V_N H_N + Q_R \tag{A10}$$

The tray hydraulic is modeled with the Francis relationship:

$$L_k = \tilde{L}_k + \frac{M_k - \tilde{M}_k}{\tau_{th}} \tag{A11}$$

where $\tilde{L}_k$ and $\tilde{M}_k$ are nominal liquid flow rate and holdup in the kth tray, respectively, and $\tau_{th} > 0$ is the hydraulic time constant.

To obtain a fully determined system, the variables appearing in these balance equations must also satisfy the following equations:

Vapor–Liquid Equilibrium

$$y_{i,j} = K_{i,j}x_{i,j} \tag{A12}$$

Summation Constrains

$$\sum_{i=1}^{N_C} x_{i,j} = 1 \qquad \forall\ j \in \mathbf{I}_N \tag{A13}$$

$$\sum_{i=1}^{N_C} y_{i,j} = 1 \qquad \forall\ j \in \mathbf{I}_N \tag{A14}$$

Thermodynamic Relations

$$K_{i,j} = k(T_j, P, \mathbf{x}_j, \mathbf{y}_j) \tag{A15}$$

$$H_j = h(T_j, P, \mathbf{y}_j) \tag{A16}$$

$$h_j = h(T_j, P, \mathbf{x}_j) \tag{A17}$$

The last three expressions can be computed from any thermodynamic method, where $\mathbf{x}_j = (x_{1,j}, x_{2,j}, \ldots, x_{N_C j})^T$ and $\mathbf{y}_j = (y_{1,j}, y_{2,j}, \ldots, y_{N_C j})^T$.

Manuscript received Jun. 13, 2002, revision received Oct. 23, 2003, and final revision received Jan. 22, 2004.